

Dalton Transactions

Accepted Manuscript



This is an *Accepted Manuscript*, which has been through the Royal Society of Chemistry peer review process and has been accepted for publication.

Accepted Manuscripts are published online shortly after acceptance, before technical editing, formatting and proof reading. Using this free service, authors can make their results available to the community, in citable form, before we publish the edited article. We will replace this *Accepted Manuscript* with the edited and formatted *Advance Article* as soon as it is available.

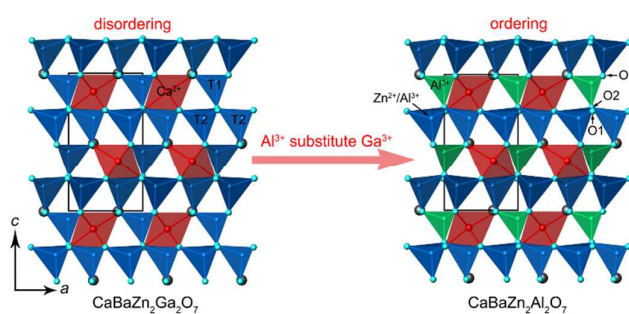
You can find more information about *Accepted Manuscripts* in the [Information for Authors](#).

Please note that technical editing may introduce minor changes to the text and/or graphics, which may alter content. The journal's standard [Terms & Conditions](#) and the [Ethical guidelines](#) still apply. In no event shall the Royal Society of Chemistry be held responsible for any errors or omissions in this *Accepted Manuscript* or any consequences arising from the use of any information it contains.

Graphical Abstract for

Structure evolution in “114” oxides $\text{CaBaZn}_2\text{Ga}_{2-x}\text{Al}_x\text{O}_7$ ($x = 0, 1, 2$) and layered cationic ordering in tetrahedral sites for $\text{CaBaZn}_2\text{Al}_2\text{O}_7$

Pengfei Jiang, Wenliang Gao, Rihong Cong, and Tao Yang



With Al³⁺ substitution, a layered type cationic ordering was observed in $\text{CaBaZn}_2\text{Al}_2\text{O}_7$, where the T1-sites are all occupied by Al³⁺.

Structure evolution in “114” oxides $\text{CaBaZn}_2\text{Ga}_{2-x}\text{Al}_x\text{O}_7$ ($x = 0, 1, 2$) and layered cationic ordering in tetrahedral sites for $\text{CaBaZn}_2\text{Al}_2\text{O}_7$

Cite this: DOI: 10.1039/x0xx00000x

Received 00th January 2012,
Accepted 00th January 2012

DOI: 10.1039/x0xx00000x

www.rsc.org/

Pengfei Jiang,^a Wenliang Gao,^a Rihong Cong,^{a*} and Tao Yang^{a*}

Rietveld refinements were performed on $\text{CaBaZn}_2\text{Ga}_{2-x}\text{Al}_x\text{O}_7$ ($x = 0, 1, 2$) in order to investigate the site preference of cations in tetrahedral cavities. Tri-valent $\text{Ga}^{3+}/\text{Al}^{3+}$ prefers the tetrahedral sites (T1-sites) within the triangular layers. And moreover, a layered type cationic ordering was observed in $\text{CaBaZn}_2\text{Al}_2\text{O}_7$, where the T1-sites are all occupied by Al^{3+} . It also represents the first example of a cationic ordering in “114” compounds. By substituting Al^{3+} into $\text{CaBaZn}_2\text{Ga}_2\text{O}_7$, the major change in structure is the shrinkage of the TlO_4 tetrahedrons, especially the shortening of the T1-O2 bond distance along the c -axis, which leads to an anisotropic shrinkage of the unit cell. In literature, such an anisotropic change of unit cell would induce a structure distortion, even a symmetry decreasing from $P6_3mc$ to $Pbn2_1$. The title compounds all crystallize in $P6_3mc$, which is unexpected. A comparison with selected “114” magnetic oxides help us to confirm that strong antiferromagnetic interactions of magnetic lattices would also be benefit to the symmetry lowering. Overall, the factors affecting cationic ordering on T1-sites and symmetry lowering are discussed upon the title compounds, which may also be applicable to other “114” oxides.

Introduction

Searching magnetic lattices showing geometrical frustration has long been an interesting subject in physics since they provide ideal models which are relevant to unusual physics in strongly correlated electronic systems, such as resonating-valence-band state proposed by Anderson in high T_C superconductors.¹ Kagomé lattice is a representative case, which is a two dimensional (2D) lattice constructed by corner-shared triangles of magnetic ions.²⁻⁴ In an ideal Kagomé lattice, the magnetic spins cannot simultaneously minimize magnetic interactions with neighbours, thus fluctuating between many different spin configurations, which usually leads to intriguing magnetic phenomena such as spin-liquid, spin-glass, and spin-ice.⁴⁻⁶

A series of oxides, which are denoted as “114” compounds with a typical formula of LnBaM_4O_7 ($\text{Ln} = \text{rare earth, Ca}; M = \text{Co, Fe, Mn, Zn, Ga, Al}$), possess an interesting crystal structure.⁷⁻¹⁷ As shown in Fig. 1, the prototype structure in the space group $P6_3mc$ has a mixed cubic-hexagonal closed packing of ionic sublattice in the form of $-\text{BaO}_3-\text{O}_4-\text{BaO}_3-\text{O}_4-$. The octahedral and tetrahedral cavities are occupied by rare-earth/alkaline-earth and transition-metal/main-group cations, respectively. The interesting point is that the tetrahedral sites can be occupied by magnetic ions, i.e. cobalt, iron and manganese, forming alternating triangular and Kagomé lattices along the c -axis (See Fig. 1). Therefore, the “114” compounds with an appropriate cationic ordering, for instance, the magnetic cations in the Kagomé layers and non-magnetic cations in the triangular layers, could be an interesting example for studying

geometrically magnetic frustration. As a representative, only a short-range coplanar magnetic ordering was observed at a very low temperature (1.2 K) in $\text{Y}_{0.5}\text{Ca}_{0.5}\text{BaCo}_4\text{O}_7$, due to the strong antiferromagnetic frustration in the Kagomé nets of Co^{2+} ($S = 3/2$), which were indeed separated by nonmagnetic triangular nets of Co^{3+} ($S = 0$).¹⁸

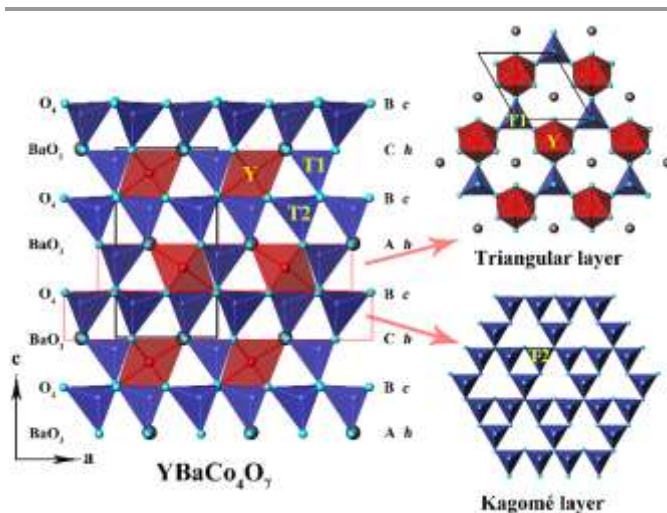


Fig. 1 A representative structure view of “114” compounds. It comprises a mixed cubic-hexagonal closed packing of “ O_4 ” and “ BaO_3 ” layers. Part of octahedral and tetrahedral cavities are occupied by Y and Co. Along the c -axis, the cations in tetrahedral cavities form triangular and Kagomé lattices alternately.

Therefore, it is interesting to investigate which factors control cationic ordering in tetrahedral sites in “114” oxides. Usually a cationic ordering in oxide materials can be induced

ARTICLE

by size and/or charge differences, as there are various examples in *A*-site or *B*-site ordered double perovskites.¹⁹⁻²² In our previous study, we obtained a non-magnetic compound $\text{CaBaZn}_2\text{Ga}_2\text{O}_7$ which belongs to the “114” family and crystallizes in $P6_3mc$.¹⁷ Here we synthesized $\text{CaBaZn}_2\text{Ga}_{2-x}\text{Al}_x\text{O}_7$ ($x = 0, 1, 2$) and investigated the structure details. Indeed, the size difference between $\text{Al}^{3+}/\text{Ga}^{3+}/\text{Zn}^{2+}$ promotes a cationic ordering, where the tetrahedral sites in triangular layers are solely occupied by Al^{3+} in $\text{CaBaZn}_2\text{Al}_2\text{O}_7$. Furthermore, we also speculated the factors influencing the crystal symmetry by comparing $\text{CaBaZn}_2\text{Ga}_{2-x}\text{Al}_x\text{O}_7$ with other magnetic “114” compounds. Those “114” compounds with a small average size of tetrahedral site cations or with strong magnetic interactions in magnetic lattices prefer a low symmetry, for example, $Pbn2_1$.

Experimental

Polycrystalline samples of $\text{CaBaZn}_2\text{Ga}_{2-x}\text{Al}_x\text{O}_7$ ($x = 0, 1, 2$) were prepared by traditional high temperature solid state reactions. Calcium carbonate (CaCO_3 , Alfa Aesar, 99.9%), barium carbonate (BaCO_3 , Alfa Aesar, 99.8%), zinc oxide (ZnO , Alfa Aesar, 99.9%), gallium oxide (Ga_2O_3 , Alfa Aesar, 99.99%) and alumina ($\gamma\text{-Al}_2\text{O}_3$, Alfa Aesar, 99.9%) were used as starting materials. All the raw materials were dried at 500 °C for 10h before weighed. Stoichiometric raw materials were mixed and ground in an agate mortar, and pre-heated at 950 °C for 10h to decompose the carbonate. After the initial calcination, the resultant powder samples were re-ground thoroughly by hands and pressed into a pellet in the diameter of 13mm. The pellet was heated at 1050~1160°C for 45h with intermediate re-grinding and re-pressing.

Powder X-ray diffraction (XRD) was performed on a Panalytical X'pert powder diffractometer equipped with a PXIcel 1D detector (Cu $K\alpha$ radiation). The operation voltage and current are 40 KV and 40 mA, respectively. The data used for phase identification were collected with a setting of 30s/0.0262°. High quality XRD data for Rietveld refinements were collected with a setting of 200s/0.0131°. Refinements were performed using the TOPAS software package.²³

Results and Discussion

Structure refinements and cationic distributions

Powder XRD patterns of $\text{CaBaZn}_2\text{GaAlO}_7$ and $\text{CaBaZn}_2\text{Al}_2\text{O}_7$ are similar with $\text{CaBaZn}_2\text{Ga}_2\text{O}_7$ (see Fig. S1 in the Electronic Supplementary Information), which proves the isomorphism. It is also apparent that the reflection peaks slightly shift to higher angles with the increase of Al^{3+} content, indicating the shrinkage of the cell lattice. Rietveld refinements were performed for all three samples in the space group $P6_3mc$. Zn^{2+} and Ga^{3+} have different cationic radii in 4-coordination (0.60 Å and 0.47 Å, respectively),²⁴ but they have almost the same scattering ability to X-ray, thus cannot be distinguished by XRD. So, during the structure refinements, Zn^{2+} and Ga^{3+} were treated as the same cation. We would analyse their respective occupancy behaviours according to the differences in

Dalton Transactions

metal-oxygen bond distances, which will be discussed in later sections. Fig. 2 gives the final refinement curves for $\text{CaBaZn}_2\text{Ga}_{2-x}\text{Al}_x\text{O}_7$ ($x = 0, 1, 2$), which all show a good convergence. Table 1 lists the refined cell parameters, atomic coordinates, occupancy factors and isotropic thermal factors.

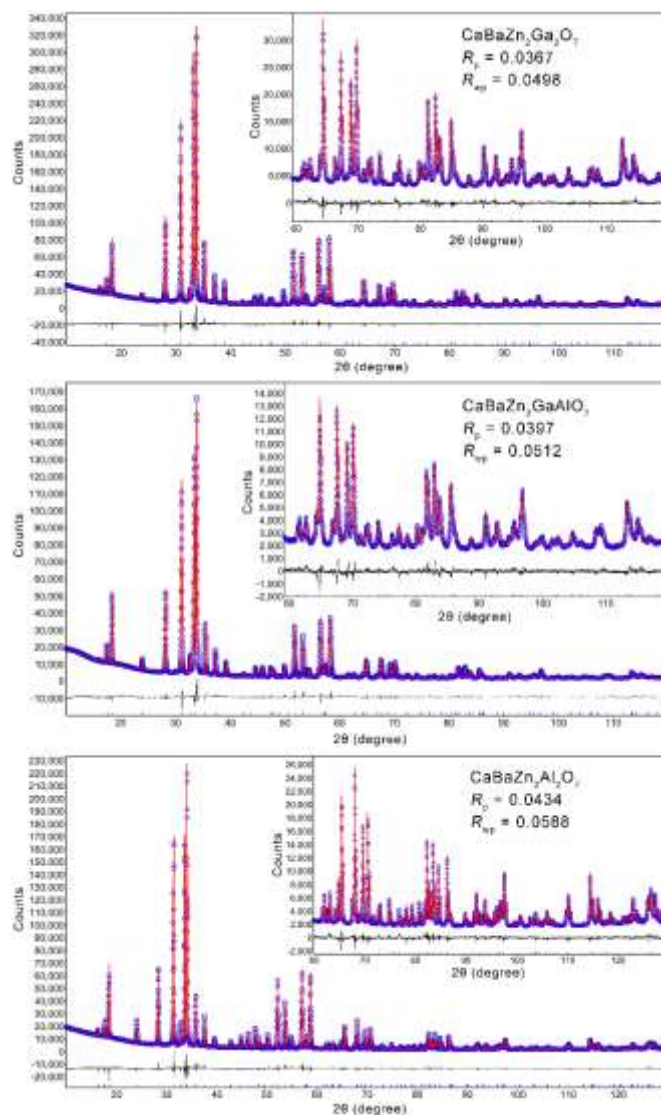


Fig. 2 The final convergence of Rietveld refinements for $\text{CaBaZn}_2\text{Ga}_{2-x}\text{Al}_x\text{O}_7$ ($x = 0, 1, 2$). The blue symbol \circ represents observed data and the red solid line is the calculated pattern; the blue marks below the diffraction patterns are the expected reflection positions, and the difference curve is also shown at the bottom. Enlargements of the high angle part are shown in the up-right corners.

During the Rietveld refinements for $\text{CaBaZn}_2\text{GaAlO}_7$, we set a constraint on the occupancy factors of Al^{3+} and $\text{Zn}^{2+}/\text{Ga}^{3+}$ at T1 (the tetrahedral site in the triangular layer) and T2 (the tetrahedral site in the Kagomé layer). For example, the occupancy of Al^{3+} at T1 and T2 were set to $1-3x$ and x , respectively. Correspondingly, the occupancy of $\text{Zn}^{2+}/\text{Ga}^{3+}$ at T1 and T2 were $3x$ and $1-x$, respectively. The refinements gave a good convergence with $x \sim 0.17$. This result indicates a preferential distribution of Al^{3+} at T1 rather than at T2 site. For $\text{CaBaZn}_2\text{Al}_2\text{O}_7$, a similar constraint was also applied at first,

Table 1. Atomic coordinates, occupancy factors, and isotropic thermal displacement parameters obtained from the Rietveld refinements. Lattice parameters for $\text{CaBaZn}_2\text{Ga}_2\text{O}_7$, $a = 6.35324(4)$ Å, $c = 10.2048(8)$ Å, $V = 356.719(5)$ Å³, $c/a = 1.606$; $\text{CaBaZn}_2\text{GaAlO}_7$, $a = 6.32539(6)$ Å, $c = 10.1208(1)$ Å, $V = 350.687(8)$ Å³, $c/a = 1.600$; $\text{CaBaZn}_2\text{Al}_2\text{O}_7$, $a = 6.29390(3)$ Å, $c = 10.02736(5)$ Å, $V = 343.999(3)$ Å³, $c/a = 1.593$.

$\text{CaBaZn}_2\text{Ga}_2\text{O}_7$	x	y	z	Occupancy	U_{eq} (Å ²)
Ca	2/3	1/3	0.8717(3)	1	0.0087(9)
Ba	2/3	1/3	0.5	1	0.0236(6)
Zn1/Ga1	0	0	0.4399(3)	1	0.0149(8)
Zn2/Ga2	0.17197(9)	0.82803(9)	0.4399(3)	1	0.0120(3)
O1	0.5057(8)	0.82803(9)	0.7392(6)	1	0.033(3)
O2	0	0	0.2531(9)	1	0.034(3)
O3	0.1589(6)	0.8411(6)	0.4916(7)	1	0.035(3)
$\text{CaBaZn}_2\text{GaAlO}_7$	x	y	z	Occupancy	U_{eq} (Å ²)
Ca	2/3	1/3		1	0.0037(8)
Ba	2/3	1/3	0.5	1	0.0016(5)
Zn1/Ga1	0	0		0.513(6)	
Al1			0.4384(5)	0.487(6)	0.005(1)
Zn2/Ga2				0.829(2)	
Al2	0.1720(1)	0.8280(1)	0.6822(2)	0.171(2)	0.0104(5)
O1	0.5071(8)	0.4929(8)	0.7368(7)	1	0.015(1)
O2	0	0	0.263(1)	1	0.022(3)
O3	0.1545(6)	0.8455(6)	0.4898(7)	1	0.029(1)
$\text{CaBaZn}_2\text{Al}_2\text{O}_7$	x	y	z	Occupancy	U_{eq} (Å ²)
Ca	2/3	1/3	0.8714(2)	1	0.0037(8)
Ba	2/3	1/3	0.5	1	0.0156(5)
Al1	0	0	0.4371(7)	1	0.005(1)
Zn2/Ga2	0.1726(1)	0.8274(1)	0.6821(2)	2/3	0.0104(5)
Al2				1/3	
O1	0.5065(7)	0.4935(7)	0.7333(7)	1	0.015(1)
O2	0	0	0.263(1)	1	0.022(3)
O3	0.1498(4)	0.8411(6)	0.4900(8)	1	0.023(3)

Table 2. Selected bond lengths obtained from Rietveld refinements for $\text{CaBaZn}_2\text{Ga}_{2-x}\text{Al}_x\text{O}_7$ ($x = 0, 1, 2$).

Bond length	$\text{CaBaZn}_2\text{Ga}_2\text{O}_7$	$\text{CaBaZn}_2\text{GaAlO}_7$	$\text{CaBaZn}_2\text{Al}_2\text{O}_7$
Ca-O1(Å) × 3	2.250(8)	2.213(8)	2.229(7)
Ca-O3(Å) × 3	2.271(7)	2.299(7)	2.327(6)
<Ca-O>(Å)	2.261	2.256	2.278
Ba-O1(Å) × 3	3.038(7)	2.966(8)	2.920(7)
Ba-O3(Å) × 6	3.1788(2)	3.1672(3)	3.1539(3)
Ba-O1(Å) × 3	3.247(7)	3.275(8)	3.273(7)
<Ba-O>(Å)	3.161	3.144	3.125
T1-O3(Å) × 3	1.832(6)	1.771(7)	1.717(5)
T1-O2(Å)	1.90(1)	1.78(1)	1.75(1)
<T1-O>(Å)	1.849	1.773	1.725
T2-O1(Å) × 2	1.911(5)	1.921(5)	1.894(5)
T2-O3(Å)	1.960(9)	1.956(8)	1.942(8)
T2-O2(Å)	2.026(4)	2.053(5)	2.049(5)
<T2-O>(Å)	1.964	1.972	1.957

and the refined occupancy factor of Al^{3+} at T1 site was 0.95, which is very close to the unit. Considering the experimental error, an ordered structure model was constructed where T1 was fully occupied by Al^{3+} , and the occupancies for Al^{3+} and $\text{Zn}^{2+}/\text{Ga}^{3+}$ at T2 sites are therefore 1/3 and 2/3, respectively (see Table 1).

The full occupancy of T1 by Al^{3+} in $\text{CaBaZn}_2\text{Al}_2\text{O}_7$ is one of the major interesting points of this work, which needs to be further verified. Therefore, a completely disordering model, where Zn and Al statistically locate at T1 and T2 sites with occupancy factor of 0.5, was built and refined with Rietveld

method. As shown in Fig. 3a, the final convergence gives the agreement factors higher than those using the ordering structure model. Moreover, the mismatch was obvious between the calculated and observed curves, for instance, the calculated intensity for the (110) reflection was higher than the observed value, while it is the opposite for the (020) reflection (see the insert of Fig. 3a). We noticed that the (110) planes contain both the T1 and T2 cations, and the (020) planes contain T1 cations (as shown in Fig. 3b). The mismatch for the (110) and (020) reflections is originated from the inappropriate scattering ability of these planes, in other words, from the wrong occupancy factors in T1 and T2 sites. By comparing the refinement results, it is confident that T1 was fully occupied by Al^{3+} in $\text{CaBaZn}_2\text{Al}_2\text{O}_7$.

Other than the occupancy factors for T1- and T2-cations, we should also pay enough attentions to the thermal displacement factors of oxygen atoms. In the current space group $P6_3mc$ we used for Rietveld refinements, there are three crystallographically independent oxygen atoms. O2 is surrounded by four cations, therefore it usually has a relatively small thermal displacement factor. O1 and O3 both locate on a mirror plane (special position 6c), and act as bridge atoms for two TO_4 tetrahedrons and one CaO_6 octahedron. If O1 and/or O3 deviated from the ideal position and the space group $P6_3mc$ was still applied, abnormal thermal factors would be observed during the refinements, which usually suggests that the real symmetry should be $P31c$, like the case in $\text{YbBaCo}_4\text{O}_7$.¹⁶ Herein our study, the obtained isotropic thermal displacement

ARTICLE

factors are all reasonable for $\text{CaBaZn}_2\text{Ga}_{2-x}\text{Al}_x\text{O}_7$ ($x = 0, 1, 2$), and as shown in Fig. 2, the differences between the observed and calculated curves are minor, indicating that $P6_3mc$ is the correct space group.

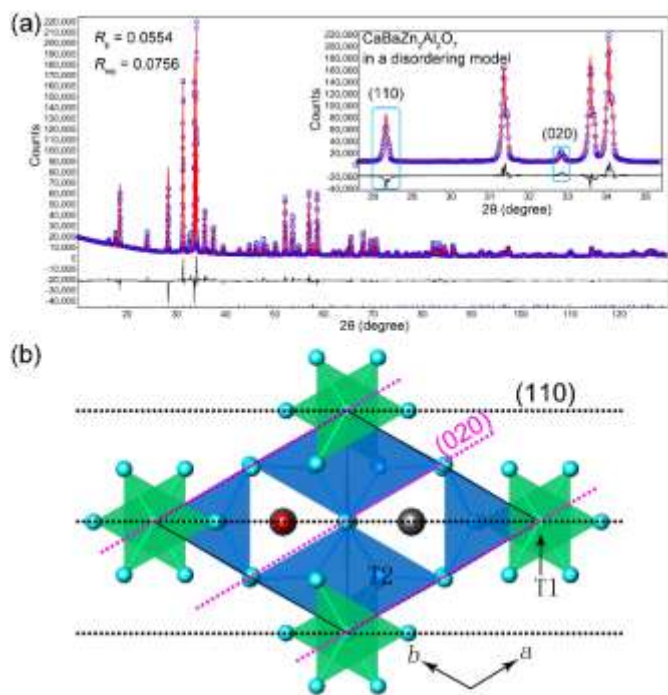


Fig. 3 (a) Final convergence of Rietveld refinements for $\text{CaBaZn}_2\text{Al}_2\text{O}_7$ in a disordering model. The insert shows an enlargement of the low angle part. The mismatch for the (110) and (020) reflections is significant; (b) a schematic view of the structure in “114” oxides, where (110) and (020) planes are highlighted. Green and blue tetrahedron are T1O_4 and T2O_4 , gray, red, cyan spheres are Ba, Ca and O, respectively.

As mentioned above, XRD cannot distinguish Zn^{2+} and Ga^{3+} . Their radii are different in 4-coordination environments, i.e. Zn^{2+} , 0.6 Å; Ga^{3+} , 0.47 Å.²⁴ Therefore, people could speculate the $\text{Zn}^{2+}/\text{Ga}^{3+}$ cationic distributions by analysing the metal-oxygen bond distances which are listed in Table 2. First, the average T1-O bond distance is significantly shorter than T2-O bond in all three compounds. In $\text{CaBaZn}_2\text{Ga}_2\text{O}_7$, the shorter T1-O bond distance suggests that the smaller cation Ga^{3+} prefers to locate on the T1 sites in the triangular layer. It should be noted that the total numbers of cations within the triangular layers are less than those within the Kagomé layers, i.e. one T1 and one Ca^{2+} cations versus three T2 cations. In such a scenario, Ga^{3+} which has a higher valence state than Zn^{2+} , tending to locate on the T1 sites is beneficial to minimize the charge difference between the triangular and Kagomé layers.

Second, the T1O_4 tetrahedrons significantly shrink along with the increase of the Al^{3+} content, for example, the average T1-O bond distance decreases from 1.849 Å to 1.725 Å. According to the Rietveld refinements, half amount of the Al^{3+} goes to T1 sites in $\text{CaBaZn}_2\text{GaAlO}_7$. And eventually a complete ordering of Al^{3+} at T1 sites was obtained in $\text{CaBaZn}_2\text{Al}_2\text{O}_7$, which ascribes to the large size difference between Al^{3+} (0.39

Å) and Zn^{2+} (0.6 Å), together with the driving force of keeping the charge neutrality between layers.

There were several examples of previously reported “114” oxides needed to be mentioned. In literature, people did not observe a layered cationic ordering in $\text{LnBaZn}_3\text{AlO}_7$ ($\text{Ln} = \text{Y}, \text{La}, \text{Nd}, \text{Sm}, \text{Eu}, \text{Gd}, \text{Dy}, \text{Lu}$)¹⁵ and $\text{YBaMn}_3\text{AlO}_7$ ⁸, which have the same and even larger size differences between Al^{3+} and $\text{Zn}^{2+}/\text{Mn}^{2+}$ sites. For example, the occupancy of Al^{3+} at T1 site was reported to be 0.3 in $\text{YBaMn}_3\text{AlO}_7$, which is even smaller than that in $\text{CaBaZn}_2\text{GaAlO}_7$. We note that the cations within the triangular layers are one T1 and one $\text{Ln}^{3+}/\text{Y}^{3+}$. By comparing to the case in $\text{CaBaZn}_2\text{Ga}_{2-x}\text{Al}_x\text{O}_7$, it becomes reasonable that the driving force of keeping the charge neutrality is also important for the cationic ordering between layers.

On the other hand, in $\text{CaBaZn}_2\text{FeAlO}_7$ and $\text{CaBaZn}_2\text{CoAlO}_7$, the T1 sites are solely occupied by trivalent $\text{Fe}^{3+}/\text{Al}^{3+}$ and $\text{Co}^{3+}/\text{Al}^{3+}$,²⁵ indicating that the T1 sites are favoured to be filled by cations with a higher valent state in CaBaM_4O_7 series. However, no cationic ordering was found for both compounds, which may due to the relatively large size of Fe^{3+} and Co^{3+} in the T1 sites.

Accordingly we speculate that the cationic size difference and keeping the charge neutrality collectively contribute to the cationic ordering. A charge ordering is observed in $\text{CaBaCo}_4\text{O}_7$ and $\text{CaBaFe}_4\text{O}_7$, where the T1 sites are fully occupied by $\text{Co}^{3+}/\text{Fe}^{3+}$.²⁶⁻²⁸ Herein our case, $\text{CaBaZn}_2\text{Al}_2\text{O}_7$ represents the first example of real cationic ordering in “114” oxides.

Structure evolution of $\text{CaBaZn}_2\text{Ga}_{2-x}\text{Al}_x\text{O}_7$ ($x = 0, 1, 2$)

The shrinkage of the unit cell volume in the solid solutions $\text{CaBaZn}_2\text{Ga}_{2-x}\text{Al}_x\text{O}_7$ ($x = 0, 1, 2$) is obvious (see Table 1) and moreover, an anisotropic change of unit cell lattice is also observed, as indicated by the decrease of c/a values (from 1.606 to 1.593). In fact, people used this c/a value of “114” oxides to evaluate the structure distortion comparing to the prototype hexagonal “114” structure in $P6_3mc$. It is known that an ideal closed packing of “ BaO_3 ” and “ O_4 ” layers gives 1.633 of c/a . For example, when the value is smaller than 1.625 in $\text{LnBaCo}_4\text{O}_7$ ($\text{Ln} = \text{Y}, \text{Er}, \text{Tm}, \text{Yb}, \text{Ho}, \text{Lu}$), the structure distortion is severe which leads to a symmetry decreasing to orthorhombic ($Pbn2_1$).²⁹ Herein, $\text{CaBaZn}_2\text{Ga}_{2-x}\text{Al}_x\text{O}_7$ ($x = 0, 1, 2$) all possess a c/a value smaller than 1.625, but crystallize in the hexagonal space group. So, it becomes interesting that there should be another factor effecting the structure symmetry of “114” oxides.

As discussed above, the major structural characteristic of $\text{CaBaZn}_2\text{Al}_2\text{O}_7$ is that the T1 sites are solely occupied by Al^{3+} , accordingly the T1O_4 tetrahedrons shrink significantly as indicated by the decrease of average T1-O bond distance from $\text{CaBaZn}_2\text{Ga}_2\text{O}_7$ to $\text{CaBaZn}_2\text{Al}_2\text{O}_7$ (see Table 2). As shown in Fig. 4, the most significant structure change by Al^{3+} -substitution can also be visualized as the wrinkling of “ O_4 ” layers comparing to original flat “ O_4 ” layers in $\text{CaBaZn}_2\text{Ga}_2\text{O}_7$. This is caused by the shortening of T1-O2 bond. For example, T1 attracts the O2 atom along the c -axis, and it also attracts O3

slightly within the *ab*-plane. Such a shrinkage of TlO_4 tetrahedrons is the main reason for the anisotropic shrinkage of

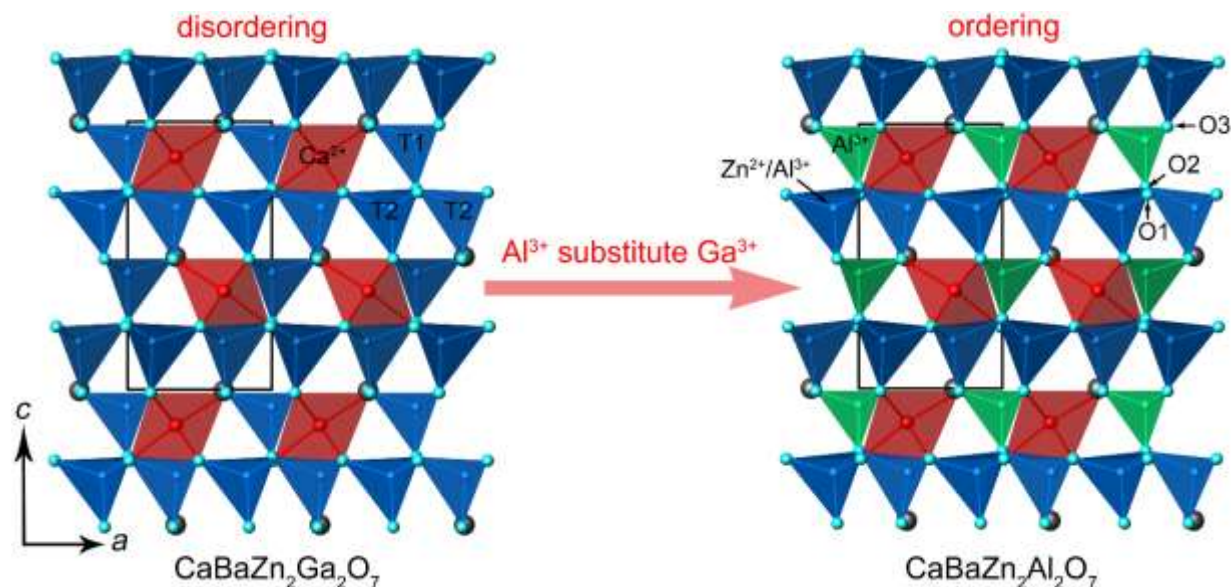


Fig. 4 Structure evolution from $\text{CaBaZn}_2\text{Ga}_2\text{O}_7$ to $\text{CaBaZn}_2\text{Al}_2\text{O}_7$. By Al^{3+} -substitution, a layered type cationic ordering was observed in $\text{CaBaZn}_2\text{Al}_2\text{O}_7$, where T-cavities in triangular layers are solely occupied by Al^{3+} . In addition, the major structure change is the shortening of T1-O2 bond distance along the *c*-axis, resulting in the wrinkling of “ O_4 ” layers.

the unit cell lattice, and therefore the decrease of *c/a* values. In other words, a smaller average size of T-cations could lead to a smaller *c/a* value and therefore a stronger structure distortion.

Average sizes of T-cations for several selected “114” oxides are given in Table 3. These oxides share a common characteristic that they possess the same ionic sub-lattices constructed by “ BaO_3 ” and “ O_4 ” layers with Ca^{2+} located in the octahedral cavities. First of all, among $\text{CaBaCo}_4\text{O}_7$, $\text{CaBaFe}_4\text{O}_7$ and $\text{CaBaZn}_2\text{Ga}_2\text{O}_7$, $\text{CaBaCo}_4\text{O}_7$ has the smallest average size of T-cation and therefore possesses the largest structure distortion in the space group $Pbn2_1$. By introducing larger cations (Zn^{2+} and Ga^{3+}) into the tetrahedral sites, the symmetry for those doped compounds $\text{CaBaCo}_{4-x}\text{Zn}_x\text{O}_7$ ($x \geq 0.8$) and $\text{CaBaCo}_{4-x}\text{Ga}_x\text{O}_7$ ($x \geq 1.0$) changes to $P6_3mc$.³⁰ It is reasonable thus far. The interesting phenomenon is that the compounds $\text{CaBaCo}_{4-x}\text{Al}_x\text{O}_7$ ($x \geq 0.4$) with smaller average T-sizes compared to $\text{CaBaCo}_4\text{O}_7$ also crystallize in the hexagonal symmetry.³¹ Accordingly we think that strong magnetic interactions within the magnetic lattices would facilitate the stabilization of an orthorhombic symmetry. For instance, a low symmetry would somehow interrupt the ideal antimagnetic frustration in a Kagomé lattice and induce a unique ground state rather than spin fluctuations. The ordered magnetic ground state occurs at low temperature, but the short-range magnetic couplings exist extensively even at room temperature. So it is a reasonable hypothesis that the strong magnetic interactions would help the compounds crystallize in a low symmetry. In Zn/Ga/Al-doped $\text{CaBaCo}_4\text{O}_7$ oxides, the magnetic interactions were weakened by non-magnetic ions substitution. So, it is not surprising that these compounds have a hexagonal symmetry ($P6_3mc$).

Back to our cases, it becomes understandable that the non-magnetic “114” compounds $\text{CaBaZn}_2\text{Ga}_{2-x}\text{Al}_x\text{O}_7$ ($x = 0, 1, 2$) all crystallize in the space group $P6_3mc$, even that $\text{CaBaZn}_2\text{Al}_2\text{O}_7$ has the smallest average T-cation size. Overall, not only the size of the T-site cations but also the magnetic interactions have an influence on the structure symmetry of the “114” oxides.

Table 3. The structure symmetry and magnetic properties of the selected “114” compounds.

Compounds	$\langle T \rangle$ size (Å)	symmetry	Low temperature magnetism
$\text{CaBaFe}_4\text{O}_7$	0.560	$P6_3mc$	ferrimagnetic
$\text{CaBaCo}_{3.2}\text{Zn}_{0.8}\text{O}_7$	0.529	$P6_3mc$	spin glass
$\text{CaBaCo}_3\text{GaO}_7$	0.526	$P6_3mc$	spin glass
$\text{CaBaCo}_{3.6}\text{Al}_{0.4}\text{O}_7$	0.517	$P6_3mc$	spin glass
$\text{CaBaCo}_4\text{O}_7$	0.525	$Pbn2_1$	ferrimagnetic
$\text{CaBaZn}_2\text{Ga}_2\text{O}_7$	0.535	$P6_3mc$	nonmagnetic
$\text{CaBaZn}_2\text{GaAlO}_7$	0.515	$P6_3mc$	nonmagnetic
$\text{CaBaZn}_2\text{Al}_2\text{O}_7$	0.495	$P6_3mc$	nonmagnetic

Conclusions

Solid solutions $\text{CaBaZn}_2\text{Ga}_{2-x}\text{Al}_x\text{O}_7$ ($x = 0, 1, 2$) were synthesized and characterized by Rietveld refinements on powder XRD data in the space group $P6_3mc$. Tri-valent cations $\text{Ga}^{3+}/\text{Al}^{3+}$ prefer to locate on the tetrahedral sites within triangular layers to balance the overall charge neutrality, and eventually the size difference between Al^{3+} and Zn^{2+} leads to a layered type cationic ordering in $\text{CaBaZn}_2\text{Al}_2\text{O}_7$. Note that $\text{CaBaZn}_2\text{Al}_2\text{O}_7$ is the first example of a layered cationic ordering in “114” oxides. By comparing our compounds to magnetic “114” oxides $\text{CaBaFe}_4\text{O}_7$, $\text{CaBaCo}_4\text{O}_7$, $\text{CaBaCo}_{4-x}\text{M}_x\text{O}_7$ ($M = \text{Zn}, \text{Ga}, \text{Al}$), we conclude that a smaller average size of T-cations would lead to a low symmetry, i.e. $Pbn2_1$. In

ARTICLE

addition, strong antimagnetic interactions would also be beneficial to the stabilization of the orthorhombic symmetry.

Acknowledgements

This work was financially supported by the Nature Science Foundation of China (Grants 91222106, 21171178) and Natural Science Foundation Project of Chongqing (Grants 2012jjA0438, 2014jcyjA50036). The Fundamental Research Funds for the Central Universities (Grant CQDXWL-2014-005) also partially supported this work. We also acknowledge the support from the sharing fund of large-scale equipment of Chongqing University.

Notes and references

^a College of Chemistry and Chemical Engineering, Chongqing University, Chongqing 400044, People's Republic of China. Corresponding author, Email: taoyang@cqu.edu.cn, congrihong@cqu.edu.cn; Tel: +86-23-65105065.

Electronic Supplementary Information (ESI) available: Powder XRD patterns for CaBaZn₂Ga_{2-x}Al_xO₇. See DOI: 10.1039/b000000x/

1. P. W. Anderson, *Science*, 1987, **235**, 1196-1198.
2. M. P. Shores, E. A. Nytko, B. M. Bartlett, D. G. Nocera, *J. Am. Chem. Soc.*, 2005, **127**, 13462-13463.
3. M. S. Williams, J. P. West, S.-J. Hwu, *Chem. Mater.*, 2014, **26**, 1502-1504.
4. S. Yan, D. A. Huse, S. R. White, *Science*, 2011, **332**, 1173-1176.
5. J. E. Greedan, *J. Mater. Chem.*, 2001, **11**, 37-53.
6. L. Balents, *Nature*, 2010, **464**, 199.
7. M. Valldor, M. Andersson, *Solid State Sci.*, 2002, **4**, 923-931.
8. M. Valldor, O. Breunig, *Solid State Sci.*, 2011, **13**, 831-836.
9. V. Pralong, V. Caignaert, A. Maignan, B. Raveau, *J. Mater. Chem.*, 2009, **19**, 8335-8340.
10. V. Caignaert, A. M. Abakumov, D. Pelloquin, V. Pralong, A. Maignan, G. Van Tendeloo, B. Raveau, *Chem. Mater.*, 2009, **21**, 1116-1122.
11. V. Caignaert, V. Pralong, A. Maignan, B. Raveau, *Solid State Commun.*, 2009, **149**, 453-455.
12. D. D. Khalyavin, L. C. Chapon, P. G. Radaelli, *Phys. Rev. B*, 2009, **80**, 144107.
13. V. Duffort, V. Caignaert, V. Pralong, A. Cervellino, D. Sheptyakov, B. Raveau, *Inorg. Chem.*, 2013, **52**, 10438-10448.
14. B. Raveau, V. Caignaert, V. Pralong, D. Pelloquin, A. Maignan, *Chem. Mater.* 2008, **20**, 6295-6297.
15. M. P. Saradhi, B. Raveau, V. Caignaert, U. V. Varadaraju, *J. Solid State Chem.*, 2010, **183**, 485-490.
16. A. Huq, J. F. Mitchell, H. Zheng, L. C. Chapon, P. G. Radaelli, K. S. Knight, P. W. Stephens, *J. Solid State Chem.*, 2006, **179**, 1136-1145.
17. P. F. Jiang, Z. X. Liu, X. R. Sun, W. L. Gao, R. H. Cong, T. Yang, *J. Solid State Chem.*, 2013, **207**, 105-110.
18. W. Schweika, M. Valldor, P. Lemmens, *Phys. Rev. Lett.*, 2007, **98**, 067201.
19. G. King, P. M. Woodward, *J. Mater. Chem.*, 2010, **20**, 5785-5796.
20. M. C. Knapp, P. M. Woodward, *J. Solid State Chem.*, 2006, **179**, 1076-1085.

Dalton Transactions

21. G. King, L. M. Wayman, P. M. Woodward, *J. Solid State Chem.*, 2009, **182**, 1319-1325.
22. T. Shimada, J. Nakamura, T. Motohashi, H. Yamauchi, M. Karppinen, *Chem. Mater.*, 2003, **15**, 4494-4497.
23. *TOPAS, V4.1-beta*, Bruker AXS, Karlsruhe, Germany, 2004.
24. R. Shannon, *Acta Crystallogr. Sect. A*, 1976, **32**, 751-767.
25. M. Valldor, *Solid State Sci.*, 2004, **6**, 251-266.
26. V. Caignaert, V. Pralong, V. Hardy, C. Ritter, B. Raveau, *Phys. Rev. B*, 2010, **81**, 094417.
27. M. M. Seikh, T. Sarkar, V. Pralong, V. Caignaert, B. Raveau, *Phys. Rev. B*, 2012, **86**, 184403.
28. N. Hollmann, M. Valldor, H. Wu, Z. Hu, N. Qureshi, T. Willers, Y. Y. Chin, J. C. Cezar, A. Tanaka, N. B. Brookes, L. H. Tjeng, *Phys. Rev. B*, 2011, **83**, 180405.
29. T. Sarkar, V. Caignaert, V. Pralong, B. Raveau, *Chem. Mater.*, 2010, **22**, 6467-6473.
30. T. Sarkar, M. M. Seikh, V. Pralong, V. Caignaert, B. Raveau, *J. Mater. Chem.*, 2012, **22**, 18043.
31. Y. M. Zou, Z. Qu, L. Zhang, W. Ning, L. S. Ling, L. Pi, Y. H. Zhang, *J. Alloy Comps.*, 2013, **576**, 1-4.